ISA Transactions xxx (xxxx) xxx

Contents lists available at ScienceDirect

ISA Transactions

journal homepage: www.elsevier.com/locate/isatrans

Practice article

Loss model based efficiency optimized control of brushless DC motor drive

Amir Khazaee [a], Hosein Abootorabi Zarchi [a,*], Gholamreza Arab Markadeh [b]

[a] Department of Electrical Engineering, Ferdowsi University of Mashhad, Mashhad, Iran
[b] Department of Engineering, Shahrekord University, Shahrekord, Iran

HIGHLIGHTS

- An accurate loss model is developed for BLDCM considering iron loss and harmonics.
- Extra iron loss due to unrequired flux at the air gap is reduced.
- Proposed method determines optimum flux corresponding to minimum loss condition.
- Model based loss minimization algorithm of BLDCM is experimentally implemented.

ARTICLE INFO

Article history:
Received 1 July 2018
Received in revised form 22 October 2018
Accepted 31 October 2018
Available online xxxx

Keywords:
Brushless DC machine
Loss model control
Loss minimization algorithm
Efficiency optimization

ABSTRACT

Energy efficiency improvement of electrical motor drives has recently become a very interesting subject. Several methods have been proposed in the literature to improve the efficiency of permanent magnet synchronous machine (PMSM) with sinusoidal back-EMF. These methods are not precise and appropriate for brushless DC machine (BLDCM) with trapezoidal back-EMF. As a unique solution, this work introduces a flux controlled based loss minimization algorithm suitable for BLDCM that considers iron loss as well as influence of back-EMF harmonics; consequently promotes efficiency of machine. In this regard, the loss model of PMSM is extended based on multiple reference frame analysis to include back-EMF harmonics of BLDCM. As an advantage, proposed modified loss model does not require any additional data about the dimensions of machine that makes it suitable for industrial motor drive applications. The Proposed loss model is validated through experimental tests in different operating conditions. Afterward, by applying direct torque and indirect flux control of BLDCM as the control technique, d-axis current in the rotor reference frame is controlled to reduce the air gap flux and consequently iron loss of the machine. Finally, a procedure is presented to determine the optimum d-axis current which maximizes the efficiency. Effectiveness of proposed control system is evaluated using simulation results in MATLAB/Simulink and experimental results on a practical prototype. It is indicated that depending on the operating conditions, about 2% to 11% of efficiency improvement would be achieved in the proposed method.

1. Introduction

The ongoing energy demand increment, environmental pollutions and limited resources have motivated efficiency improvements in all fields of engineering. Electric motors consume almost 50% of the electricity generated around the world [1]. Accordingly, any minor improvement in operating efficiency of motors, would significantly reduce global consumed energy, decrease greenhouse gas emissions and reduce depletion rate of the resources. Brushless DC machines (BLDCM) are popular in industrial applications due to their high efficiency, high torque density and reliability [2]. Most studies in the field of BLDCM drive have mostly focused on torque ripple reduction. These efforts are generally based on optimal shaping of stator currents [3,4] or using direct torque control (DTC) system [5]; however, in many industrial applications such as pumps, fans, compressors and renewable energy systems, torque ripples may not be the major criteria and the efficiency is more important. For instance, in a recent developed control system for permanent magnet synchronous machine (PMSM) [6], higher efficiency is achieved with the penalty of torque ripple increment.

The efficiency of BLDCM is relatively high in the variety of torque–speed range and hence it is a good candidate for variable speed, long time applications like electric vehicles, pumps and fans; however, efficiency of the machine, can be improved in the machine design procedure [7]. Afterward for an existing machine, the efficiency optimization can be achieved by a controlling strategy.

* Corresponding author.
E-mail addresses: amir.khazaee@mail.um.ac.ir (A. Khazaee), abootorabi@um.ac.ir (H. Abootorabi Zarchi), arab-gh@eng.sku.ac.ir (G. Arab Markadeh).

https://doi.org/10.1016/j.isatra.2018.10.046
0019-0578/

Nomenclature

Abbreviations

BLDCM	Brushless direct current machine
PMSM	Permanent magnet synchronous machine
EMF	Electromotive force
DTC	Direct torque control
LMA	Loss minimization algorithms
MRF	Multiple reference frame
MTPA	Maximum torque per ampere

Symbols

R_s	Phase resistance
R_c	Equivalent iron loss resistance
L	Stator inductance
P	Number of pole pairs
k_n	Normalized magnitude of nth harmonic relative to fundamental
k_h, k_e	Hysteresis and Eddy current loss coefficients
ω_r	Rotor electrical speed
ω_m	Rotor mechanical speed
θ_r	Rotor electrical position
T_e	Electromagnetic torque
λ'_{m}	Flux linkage established by magnets
B_m	Peak value of flux density
B	Viscosity coefficient
i^r_{qs}, i^r_{ds}	q- and d-axis currents in rotor reference frame
i^{xr}_{qs}, i^{xr}_{ds}	Transformation of i^r_{qs}, i^r_{ds} into a reference frame rotating at x times of rotor electrical speed i^r_{cq}, i^r_{cd} q- and d-axis core loss armature currents
P_{Cu}	Resistive loss
P_{FE}	Iron loss
P_{Mech}	Mechanical loss
P_{Loss}	Total loss
v^r_{qs}, v^r_{ds}	q- and d-axis voltages in rotor reference frame
v^{xr}_{qs}, v^{xr}_{ds}	Transformation of v^r_{qs}, v^r_{ds} into a reference frame rotating at x times of rotor electrical speed

Efficiency optimization of BLDCM drive system has been addressed in several researches [8–12]. In this regard a numeric method has been suggested by Hanselman to minimize a cost function that includes torque ripple and stator resistive loss [8]. With similar objectives, Aghili, et al. proposed quadratic programming-based control of a multiphase BLDCM by injecting harmonic currents to the stator [9]. In [10] authors developed an optimal feedback linearization control that works at varying torque–speed range and resistive loss has been claimed to be minimized. Iron loss as a key parameter on efficiency has not been considered in these papers. In [11] a simple strategy to determine optimum current excitation considering non-ideal and unbalanced back-EMF waveforms has been reported. Although complicated calculations of harmonic coefficients have been effectively reduced, iron loss has not been taken into account.

Kshirsagar and Krishnan stated that BLDCM tends to have higher iron loss owing to back-EMF harmonics [12]; therefore, underestimating iron loss would be an unreasonable choice which degrades the system performance in efficiency maximization study. Authors used an analytical approach for iron loss calculation and compared various stator current injection strategies. Finally, they suggested a hybrid control strategy in which, non-sinusoidal harmonic injection scheme is used in the speed range, until the sum of inverter conduction and stator resistive loss exceeds iron loss. When iron loss becomes dominant, the sinusoidal currents are preferred. Calculation of the iron loss in this method requires accurate data of machine dimensions which is not available in many cases. Table 1 provides a comparison of researches in topic of BLDCM efficiency optimization, including methodologies, improvements, and features.

Generally machines are designed for their highest efficiency at rated conditions. However, in many applications, they are usually run under light loading conditions. In conventional constant flux control system, extra iron loss would be emerged due to an unrequired flux linkage. There exists an optimum point for flux where the efficiency is maximum. In the literature, the term 'loss minimization algorithm (LMA)' refers to control strategies, minimizing total power loss by determining the optimum flux level. LMAs in electrical drives can be categorized into two groups: model-based and online search-based loss control. Model-based loss control is based on mathematical development of loss model of machine and requires a precise model. Search-based loss control, on the contrary, is an adaptive but time-consuming approach [14]. Several researchers addressed model-based LMA for sinusoidal PMSM [13,15]. Such approaches could not be employed for BLDCM with trapezoidal back-EMF. An alternative loss model is mandatory to include back-EMF harmonics.

In this paper the loss model of PMSM is modified for BLDCM based on multiple reference frame (MRF) theory. The advantage of the modified loss model is that the iron loss, influence of back-EMF harmonics and variation of the iron loss resistance are considered. Moreover it does not require any additional data about dimensions of machine, making it suitable in industrial motor drive applications. The proposed model is evaluated through experiments in multiple operating conditions. Afterward by applying direct torque and indirect flux control of BLDCM, reported in [16], a simple control strategy for minimizing total loss of machine is provided. In this method, d-axis current in the rotor reference frame is controlled in order to reduce the air gap flux and consequently the iron loss of the machine. Finally, a procedure for determining the optimum d-axis current that maximizes the efficiency is presented.

As a unique solution for LMA of BLDCM, contributions of this paper could be summarized as follows:

- Modified loss model of BLDCM is developed based on MRF theory to include iron loss and influence of the back-EMF harmonics without information about the machine characteristics and dimensions.
- Due to sharp changes in stator flux locus whose amplitudes are unpredictable, flux control operation of BLDCM which is the basis of LMA would not be feasible in the conventional two-phase conduction mode [17]. Consequently previous studies made no attempt to control the stator flux of BLDCM at its optimum point. In this paper, the optimum flux control operation is achieved employing direct torque and indirect flux control approach. In other words, in this research extra iron loss due to unrequired flux could be removed by efficient control of the flux at its optimum value.

Please cite this article as: A. Khazaee, H. Abootorabi Zarchi and G. Arab Markadeh Loss model based efficiency optimized control of brushless DC motor drive. ISA Transactions (2018), https://doi.org/10.1016/j.isatra.2018.10.046.

Table 1
Comparison of efficiency optimization approaches for BLDCM.

Ref.	Motor rating	Improvement	Iron loss considered?	Influence of harmonics considered?
[9]	1.5k W	20% increment of maximum torque	No	Yes
[10]	830 W	Up to 8.2% reduction of power loss	No	No
[11]	400 W	Efficiency improvement is not mentioned	No	Yes
[12]	200 W	2%–5% efficiency improvement	Yes (requires dimensions)	Yes
[13]	3.5 kW	2%–18% efficiency improvement	Yes	No
Present work	200 W	2%–11% efficiency improvement	Yes	Yes

- A simple control strategy is proposed and experimentally implemented to determine the optimum flux level corresponds to minimum loss condition at any operational point.

The rest of the paper organized as follows. A description on machine modeling using MRF theory and modified loss model are provided in Sections 2 and 3. The method of choosing the optimum *d*-axis current in the rotor reference frame through proposed LMA is discussed in Section 4. The provided outputs in the MATLAB/Simulink platform as well as the experimental results on a 200 W prototype, validate the effective performance of the proposed control system in several operating points

2. Machine modeling and description

In order to derive a useful model for machine drive systems, the machine model must put into a form which does not have any rotor position dependent terms in variables and also the variables are constant at steady state. Although an ideal model for sinusoidal PMSM can be derived by using the Park transformation, it is not valid for BLDCM with non-sinusoidal back-EMF; therefore, an alternate analysis is mandatory. Such an analysis, is proposed by Chapman, et al. using MRF theory [18].

It is assumed that BLDCM is of surface-mounted type and stator windings are wye connected to eliminate circulating the third harmonic currents. For an ideal trapezoidal back-EMF with 240° of flat area per cycle, 99% of power belongs to the first seven harmonics [18]. Therefore the harmonics of more than 7th are not considered in model. In addition, owing to wye connection with floating neutral of stator windings, triple harmonics of stator currents would not be circulated. Thus 5th and 7th harmonics are only considered in the analysis.

Initially, the stator variables are transferred into the rotor reference frame by applying Park transformation as presented in Eq. (1) and the electromagnetic torque is obtained as follows [19].

$$\begin{cases} v_{qs}^{r} = R_s i_{qs}^{r} + L\frac{di_{qs}^{r}}{dt} + \omega_r L i_{ds}^{r} + \omega_r \lambda'_m[1 + (5k_5 + 7k_7)\cos(6\theta_r)] \\ v_{ds}^{r} = R_s i_{ds}^{r} + L\frac{di_{ds}^{r}}{dt} - \omega_r L i_{qs}^{r} + \omega_r \lambda'_m[(5k_5 - 7k_7)\sin(6\theta_r)] \end{cases} \tag{1}$$

$$T_e = 1.5P\lambda'_m[i_{qs}^{r} + (5k_5 + 7k_7)\cos(6\theta_r)i_{qs}^{r} + (5k_5 - 7k_7)\sin(6\theta_r)i_{ds}^{r}] \tag{2}$$

It is observed that in the rotor reference frame, the stator voltage and electromagnetic torque equations, contain $6\theta_r$-dependent terms due to relative speed between fundamental component and 5th and 7th harmonics, rotating in the negative and positive directions respectively.

MRF analysis is then used to transfer state variables from rotor reference frame to another reference frame, rotating at 5th and 7th multiples of rotor speed. This results in removing $6\theta_r$-dependent terms of variables. By applying following transformation on Eqs. (1), (2) the electromagnetic torque is derived as follows

$$f_{qd}^{xr} = \begin{bmatrix} \cos(x\theta_r - \theta_r) & -\sin(x\theta_r - \theta_r) \\ \sin(x\theta_r - \theta_r) & \cos(x\theta_r - \theta_r) \end{bmatrix} f_{qd}^{r} \tag{3}$$

$$T_e = 1.5P\lambda'_m[i_{qs}^{r} + 5k_5 i_{qs}^{-5r} + 7k_7 i_{qs}^{7r}] \tag{4}$$

where f_{qd}^{xr} denotes the transformation of currents, voltages or flux linkages into a reference frame rotating at x times of the electrical speed. In order to find i_{qs}^{-5r} and i_{qs}^{7r}, this transformation should be applied to Eq. (1) to establish transformed voltage equation for harmonic components. Additionally an averaging procedure should be taken over $2\pi/6$ increment of electrical rotor position to remove $6\theta_r$-dependent terms [18]. Finally, the expression of the voltages and torque dynamics can be defined as follows:

$$\begin{cases} \bar{v}_{qs}^{r} = R_s \bar{i}_{qs}^{r} + L\frac{d\bar{i}_{qs}^{r}}{dt} + \omega_r L \bar{i}_{ds}^{r} + \omega_r \lambda'_m \\ \bar{v}_{ds}^{r} = R_s \bar{i}_{ds}^{r} + L\frac{d\bar{i}_{ds}^{r}}{dt} - \omega_r L \bar{i}_{qs}^{r} \\ \bar{v}_{qs}^{-5r} = R_s \bar{i}_{qs}^{-5r} + L\frac{d\bar{i}_{qs}^{-5r}}{dt} - 5\omega_r L \bar{i}_{ds}^{-5r} + 5k_5\omega_r \lambda'_m \\ \bar{v}_{ds}^{-5r} = R_s \bar{i}_{ds}^{-5r} + L\frac{d\bar{i}_{ds}^{-5r}}{dt} + 5\omega_r L \bar{i}_{qs}^{-5r} \\ \bar{v}_{qs}^{7r} = R_s \bar{i}_{qs}^{7r} + L\frac{d\bar{i}_{qs}^{7r}}{dt} + 7\omega_r L \bar{i}_{ds}^{7r} + 7k_7\omega_r \lambda'_m \\ \bar{v}_{ds}^{7r} = R_s \bar{i}_{ds}^{7r} + L\frac{d\bar{i}_{ds}^{7r}}{dt} - 7\omega_r L \bar{i}_{qs}^{7r} \end{cases} \tag{5}$$

$$T_e = 1.5P\lambda'_m[\bar{i}_{qs}^{r} + 5k_5 \bar{i}_{qs}^{-5r} + 7k_7 \bar{i}_{qs}^{7r}] \tag{6}$$

where $\bar{f}$ denotes average value of f over $2\pi/6$ increment of electrical rotor position.

Thus far, the desired model is derived based on MRF analysis. Although in this model the number of state variables is increased, they are independent and constant in steady state operation. It is worth mentioning that current MRF analysis did not consider the effects of the iron loss. As described in the next section, the previous study has been developed in the present paper to include the iron loss into study.

3. Modified loss model of BLDCM based on MRF

As it mentioned earlier, there are two types of loss minimization algorithms: model based and search based algorithms. Among them, model based algorithms require a precise model but have the advantage of faster response and less torque ripple. In this paper, loss model of PMSM is modified to include back-EMF harmonics of BLDCM. Proposed modified loss model is based on MRF analysis and promotes the accuracy and performance of BLDCM loss minimization algorithm.

3.1. Loss model of PMSM

Stator voltage dynamic equations of PMSM in rotor reference frame are as follows,

$$\begin{cases} v_{qs}^{r} = R_s i_{qs}^{r} + L\frac{di_{oq}^{r}}{dt} + \omega_r L i_{od}^{r} + \omega_r \lambda'_m \\ v_{ds}^{r} = R_s i_{ds}^{r} + L\frac{di_{od}^{r}}{dt} - \omega_r L i_{oq}^{r} \end{cases} \tag{7}$$

where

$$i_{cd}^{r} = i_{ds}^{r} - i_{od}^{r} \quad i_{cq}^{r} = i_{qs}^{r} - i_{oq}^{r} \tag{8}$$

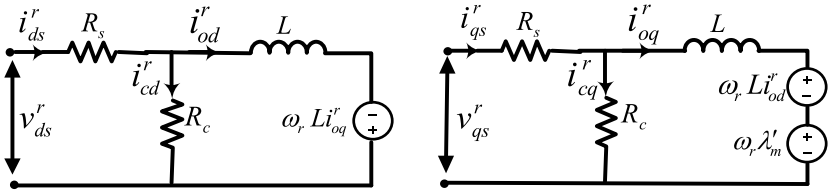

Fig. 1. Equivalent circuit of PMSM including iron loss.

$$i^r_{cd} = \frac{Ldi^r_{od}/dt - Li^r_{oq}\omega_r}{R_c} \tag{9}$$

$$i^r_{cq} = \frac{Ldi^r_{oq}/dt + Li^r_{od}\omega_r + \lambda'_m\omega_r}{R_c}. \tag{10}$$

Loss model development and implementation of loss minimization algorithm for sinusoidal PMSM is reported in [13]. The equivalent circuit of PMSM, in which iron loss is included as the iron loss resistance (R_c) is shown in Fig. 1. The value of R_c is calculated from

$$R_c = \frac{e^2_{rms}}{P_{FE}} \tag{11}$$

where e_{rms} is RMS value of back-EMF and P_{FE} is iron loss of machine [20] and would be found as

$$P_{FE} = k_h\omega_m B^n_m + k_e\omega^2_m B^2_m \tag{12}$$

where k_h, k_e and n are constants, could be obtained from manufacturer datasheets or parameter identification methods. e_{rms} is proportional to the product of rotor speed and flux density i.e. $e_{rms} = C\omega_m B_m$; moreover, usually $n = 2$ [21]. Therefore, equivalent iron loss resistance would be obtained by

$$R_c = \frac{1}{k'_e + k'_h/\omega_m} \tag{13}$$

where$k'_h = c_1 k_h$ and $k'_e = c_2 k_e$ and c_1, c_2 are constants [6]. PMSM loss in steady state can be found as

$$P_{Loss} = P_{Cu} + P_{FE} + P_{Mech} = 1.5R_s(i^{r^2}_{qs} + i^{r^2}_{ds}) + 1.5R_c(i^{r^2}_{cq} + i^{r^2}_{cd}) + B\omega^2_m. \tag{14}$$

Afterward, in order to minimize the electrical loss, the optimum value for flux linkage in which the electrical loss is minimum will be obtained.

3.2. Modified loss model of BLDCM

Unlike sinusoidal PMSM, the back-EMF of BLDCM is trapezoidal and contains harmonics. The harmonics of back-EMF also produce iron loss [22]; therefore, the electrical loss of PMSM is not precise here for BLDCM. MRF analysis is used in this paper to find a more accurate model of electrical loss in BLDCM in presence of harmonics. As previously discussed, only 5th and 7th harmonics are considered. It is observed in dynamic equations of BLDCM in Eq. (5) that there exist three sets of equations belong to fundamental component, 5th and 7th harmonics. Each set, specifies dynamic equation of its harmonic order; therefore, including iron loss into the model, leads to an equivalent circuit for each set as indicated in Fig. 2. In this scheme, impact of iron loss of fundamental component and 5th and 7th harmonics are represented by three equivalent iron loss resistances (R_{c1}, R_{c5} and R_{c7}). These parameters can be obtained based on Eqs. (11)–(13) as follows

$$R_{ci} = \frac{e^2_{rms,i}}{k'_e e^2_{rms,i} + k'_h e^2_{rms,i}/i\omega_m} = \frac{1}{k'_e + k'_h/i\omega_m} \tag{15}$$

where i denotes for ith harmonic component. The equivalent loss resistance is usually considered to be constant and is calculated in rated condition. In this paper the influence of loss resistance variation is considered by measuring it at various operating points experimentally and saving it as a look-up table.

Regarding Fig. 2, total loss of BLDCM can be determined as follows,

$$\begin{aligned} P_{Loss} &= P_{Cu} + P_{FE} + P_{Mech} = 1.5R_s(\bar{i}^{r^2}_{qs} + \bar{i}^{r^2}_{ds}) + 1.5R_{c1}(\bar{i}^{r^2}_{cq} + \bar{i}^{r^2}_{cd}) \\ &+ 1.5R_s(\bar{i}^{-5r^2}_{qs} + \bar{i}^{-5r^2}_{ds}) + 1.5R_{c5}(\bar{i}^{-5r^2}_{cq} + \bar{i}^{-5r^2}_{cd}) \\ &+ 1.5R_s(\bar{i}^{7r^2}_{qs} + \bar{i}^{7r^2}_{ds}) + 1.5R_{c7}(\bar{i}^{7r^2}_{cq} + \bar{i}^{7r^2}_{cd}) + B\omega^2_m \end{aligned} \tag{16}$$

where steady state iron loss components of dq-axis currents are calculated from Eqs. (17)–(19).

$$\bar{i}^r_{cd} = \frac{-L\bar{i}^r_{oq}\omega_r}{R_{c1}}, \qquad \bar{i}^r_{cq} = \frac{L\bar{i}^r_{od}\omega_r + \lambda'_m\omega_r}{R_{c1}} \tag{17}$$

$$\bar{i}^{-5r}_{cd} = \frac{5L\bar{i}^{-5r}_{oq}\omega_r}{R_{c5}}, \qquad \bar{i}^{-5r}_{cq} = \frac{-5L\bar{i}^{-5r}_{od}\omega_r + 5k_5\lambda'_m\omega_r}{R_{c5}} \tag{18}$$

$$\bar{i}^{7r}_{cd} = \frac{-7L\bar{i}^{7r}_{oq}\omega_r}{R_{c7}}, \qquad \bar{i}^{7r}_{cq} = \frac{7L\bar{i}^{7r}_{od}\omega_r + 7k_7\lambda'_m\omega_r}{R_{c7}}. \tag{19}$$

In order to find steady state iron loss components of dq-axis currents from motor terminal variables (which are simply available by sensors), by expanding $\bar{i}^r_{oq}$, $\bar{i}^r_{od}$ based on Eq. (8) some manipulations are required as follows

$$\begin{aligned} \bar{i}^r_{cd} &= \frac{-L\omega_r}{R_{c1}}(\bar{i}^r_{qs} - \bar{i}^r_{cq}) \\ &= \frac{-L\omega_r}{R_{c1}}(\bar{i}^r_{qs} - (\frac{L(\bar{i}^r_{ds} - \bar{i}^r_{cd})\omega_r + \lambda'_m\omega_r}{R_{c1}})) \\ &= \frac{-L\omega_r R_{c1}\bar{i}^r_{qs} + \omega^2_r L\lambda'_m + \omega^2_r L^2\bar{i}^r_{ds}}{R^2_{c1} + \omega^2_r L^2} \end{aligned} \tag{20}$$

$$\begin{aligned} \bar{i}^r_{cq} &= \frac{\lambda'_m\omega_r}{R_{c1}} + \frac{L\omega_r}{R_{c1}}(\bar{i}^r_{ds} - \bar{i}^r_{cd}) \\ &= \frac{\lambda'_m\omega_r}{R_{c1}} + \frac{L\omega_r}{R_{c1}}\bar{i}^r_{ds} + \frac{L^2\omega^2_r}{R^2_{c1}}(\bar{i}^r_{qs} - \bar{i}^r_{cq}) \\ &= \frac{L\omega_r R_{c1}\bar{i}^r_{ds} + R_{c1}\omega_r\lambda'_m + \omega^2_r L^2\bar{i}^r_{qs}}{R^2_{c1} + \omega^2_r L^2} \end{aligned} \tag{21}$$

Similar manipulations could be applied to Eqs. (18)–(19) to find harmonic components as follows:

$$\bar{i}^{-5r}_{cd} = \frac{5L\omega_r R_{c5}\bar{i}^{-5r}_{qs} - 25\omega^2_r Lk_5\lambda'_m - 25\omega^2_r L^2\bar{i}^{-5r}_{ds}}{R^2_{c5} + 25\omega^2_r L^2} \tag{22}$$

$$\bar{i}^{-5r}_{cq} = \frac{-5L\omega_r R_{c5}\bar{i}^{-5r}_{ds} + 5k_5 R_{c5}\omega_r\lambda'_m + 25\omega^2_r L^2\bar{i}^{-5r}_{qs}}{R^2_{c5} + 25\omega^2_r L^2} \tag{23}$$

$$\bar{i}^{7r}_{cd} = \frac{-7L\omega_r R_{c7}\bar{i}^{-7r}_{q} + 49\omega^2_r Lk_7\lambda'_m + 49\omega^2_r L^2\bar{i}^{7r}_{d}}{R^2_{c7} + 49\omega^2_r L^2} \tag{24}$$

Please cite this article as: A. Khazaee, H. Abootorabi Zarchi and G. Arab Markadeh Loss model based efficiency optimized control of brushless DC motor drive. ISA Transactions (2018), https://doi.org/10.1016/j.isatra.2018.10.046.

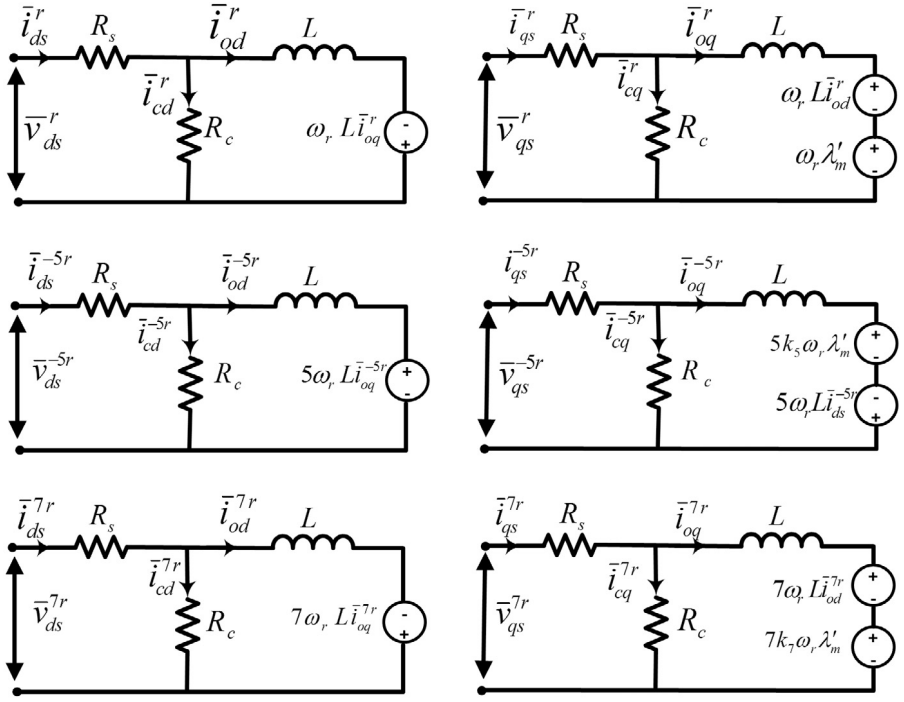

Fig. 2. Equivalent circuit of BLDCM including iron loss.

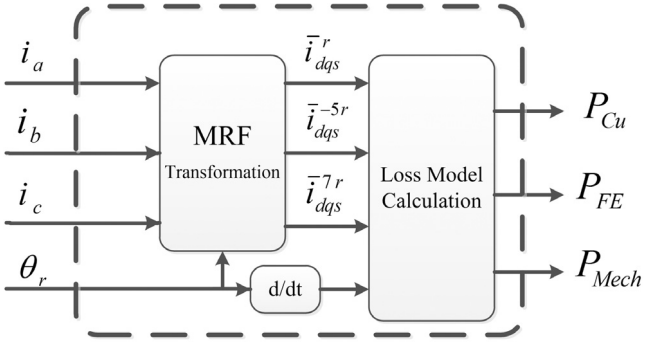

Fig. 3. Modified loss model of BLDCM.

$$\bar{i}^{7r}_{cq} = \frac{7L\omega_r R_{c7}\bar{i}^{7r}_{ds} + 7k_7 R_{c7}\omega_r\lambda'_m + 49\omega_r^2 L^2\bar{i}^{7r}_{qs}}{R_{c7}^2 + 49\omega_r^2 L^2}. \quad (25)$$

Such far, total loss of BLDCM is achieved by applying MRF transformation on sensed terminal currents, calculating steady state iron loss components of d*q*-axis currents through Eqs. (20)–(25), and substituting these variables into Eq. (16). Fig. 3 shows the block diagram of modified loss model of BLDCM. Validity of proposed modified loss model would be examined through experiments in Section 6.

4. Proposed efficiency optimized control system for BLDCM

In the conventional constant flux control system, extra iron loss would be emerged due to unrequired flux linkage. There exists an optimum point for the flux where efficiency is maximum. In the so called 'loss minimization algorithms', it is possible to reduce the loss of machine, by efficient control of the flux linkage. Researchers have developed several methods of LMA for induction machine [23] and sinusoidal PMSM [15]. In reviewing the literature, no approach was found on LMA of BLDCM because of challenges of flux control operation. In this paper following approach which has been introduced previously in [16] for flux weakening region in high speed operation, is employed to control the flux at its optimum value.

4.1. Direct torque and indirect flux control of BLDCM

It is stated in [17] that flux linkage cannot be controlled in two-phase conduction mode because of sharp changes whose amplitudes are unpredictable in stator flux locus. Authors proposed direct torque and indirect flux control of BLDCM in [16] for three-phase conduction mode. In this method torque is directly controlled where flux linkage is indirectly controlled by amplitude of *d*-axis current in rotor reference frame. Fig. 4 shows the block diagram of control system. Switching table for direct torque and indirect flux control system is given in Table 2, in which φ and τ are the outputs of the flux and torque hysteresis comparators respectively. The value of "−1" for φ and τ means that actual value is above the reference value and out of the hysteresis limit and vice versa. Instead of flux itself, the *d*-axis current control is used. Additionally, the position of rotor could be estimated from flux linkage yields to an improved reliability with reduced expenses control drive system [24,25].

In [16] the set point of *d*-axis current has been kept at zero in constant torque region which means constant flux linkage operation. The flux control operation has been applied only in flux weakening region for higher speed. In the current study, set point of *d*-axis current is determined to minimize loss of machine.

4.2. Proposed loss minimization algorithm

Herein, the optimal value of *d*-axis current where sum of resistive, iron and mechanical loss is minimum should be obtained. A common way to find it, is differentiating P_{loss} obtained from Eq. (16) with respect to *d*-axis current and equating it to zero as

$$\frac{\partial P_{Loss}}{\partial i^r_{ds}} = 0. \quad (26)$$

Please cite this article as: A. Khazaee, H. Abootorabi Zarchi and G. Arab Markadeh Loss model based efficiency optimized control of brushless DC motor drive. ISA Transactions (2018), https://doi.org/10.1016/j.isatra.2018.10.046.

Table 2
Switching table for direct torque and indirect flux control of BLDCM.

φ	τ	Sector					
		1	2	3	4	5	6
1	1	V2(110)	V3(010)	V4(011)	V5(001)	V6(101)	V1(100)
	−1	V6(101)	V1(100)	V2(110)	V3(010)	V4(011)	V5(001)
−1	1	V3(010)	V4(011)	V5(001)	V6(101)	V1(100)	V2(110)
	−1	V5(001)	V6(101)	V1(100)	V2(110)	V3(010)	V4(011)

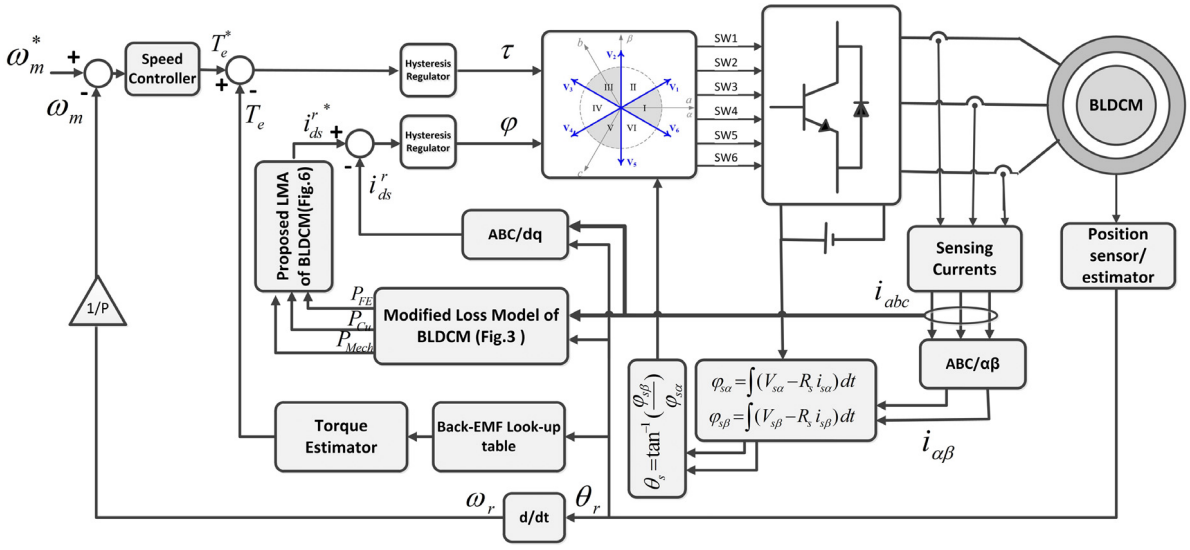

Fig. 4. Overall block diagram of proposed LMA control system.

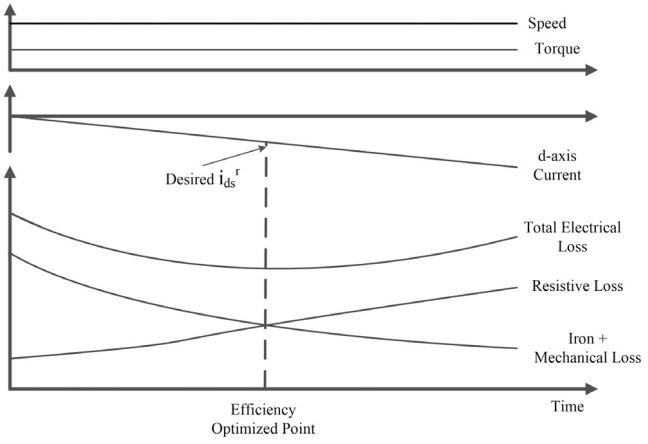

Fig. 5. Principle of LMA.

However, it is very complicated to be solved and is not proper for real-time control systems. Fig. 5 shows the principle of LMA for permanent magnet equipped motors [26]. At the beginning, due to existence of permanent magnets in rotor, the iron loss is dominant; therefore, in constant flux operation, the iron loss is relatively high. By reducing the flux linkage (increasing the magnitude of i^r_{ds}), the iron loss is decreased while resistive loss is increased. Therefore, in a specified torque–speed condition, the minimum loss, corresponds to a specified point where sum of iron and mechanical loss meets resistive loss. This criterion is used in this paper to obtain the maximum efficiency point of BLDCM.

Fig. 6 shows proposed LMA algorithm flowchart. The algorithm searches for optimum value of i^r_{ds} in which total loss is minimum through loss model of BLDCM.

The initial value for *d*-axis current is assumed to be zero. Afterward the resistive, iron and mechanical losses would be calculated by using motor speed and sensed currents that are transformed by MRF transformation (Fig. 3). The difference between iron plus mechanical loss and resistive loss (dP) is the criteria of the decision. If the sum of iron and mechanical loss is dominant, the reference value of *d*-axis current (i^{r*}_{ds}) will be increased with predefined step amplitude (di_d) and vice versa. In order to improve the response time of the controller, a variable gain is multiplied by the step function. This gain is relatively high where dP is high. By decreasing dP, the gain can be decreased too. Experimental and simulation results in the next section validate suitable performance of the proposed strategy.

It should be noted that similar to other model based loss minimization techniques, efficiency improvement of machine requires precise parameters; therefore, variation of inductances as well as stator resistance could be considered for improvement of accuracy. However these are left for future research studies.

5. Simulation results

Performance of the developed DTC based LMA is now validated through simulations in MATLAB/SIMULINK software for a 3-phase 200 W BLDCM specified in Table 3.

The ability of controlling flux linkage of BLDCM, which is the basis of LMA, is indicated in Fig. 7. In this assessment, i^{r*}_{ds} is changed from 0 A to −3.4 A at the rated speed (30 rad/s) and 50% of load torque (3.3 Nm). It is clearly observed that the magnitude of the stator flux linkage is indirectly controlled properly by controlling the *d*-axis current. In addition, the stator flux linkage locus has dodecagon shape due to trapezoidal waveform of the back-EMF. Fig. 8 shows the simulation results of BLDCM when speed command is set at its rated value (30 rad/s) for stepwise changes in the load torque (Fig. 8(a)). Proposed LMA is applied at the time

Please cite this article as: A. Khazaee, H. Abootorabi Zarchi and G. Arab Markadeh Loss model based efficiency optimized control of brushless DC motor drive. ISA Transactions (2018), https://doi.org/10.1016/j.isatra.2018.10.046.

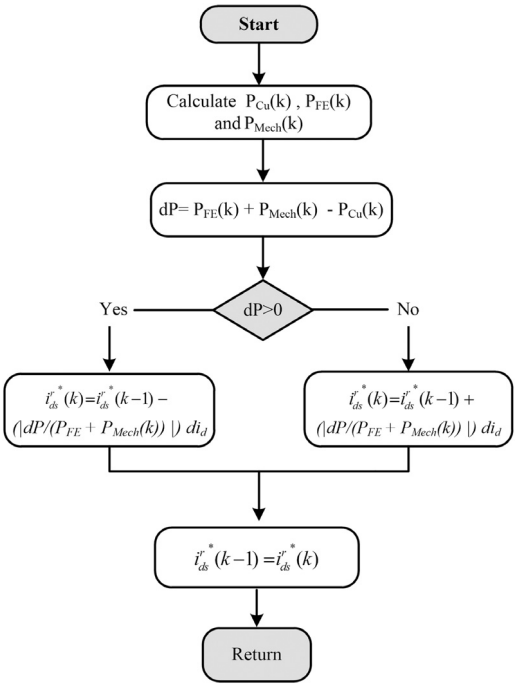

Fig. 6. Proposed LMA algorithm.

Table 3
Machine parameters.

Rated speed (rad/s)	30
Rated torque (Nm)	6.6
Rated Voltage (V)	24
P, Number of pole pairs	8
R_s (Ω)	0.56
L (mH)	1.24
λ'_m (wb)	0.07627
J, Rotor inertia constant (Kg.m^2)	0.37e−2
B, Friction coefficient (Nm/rad/s)	0.94e−3
k'_h, k'_e	0.0198, 0.08695

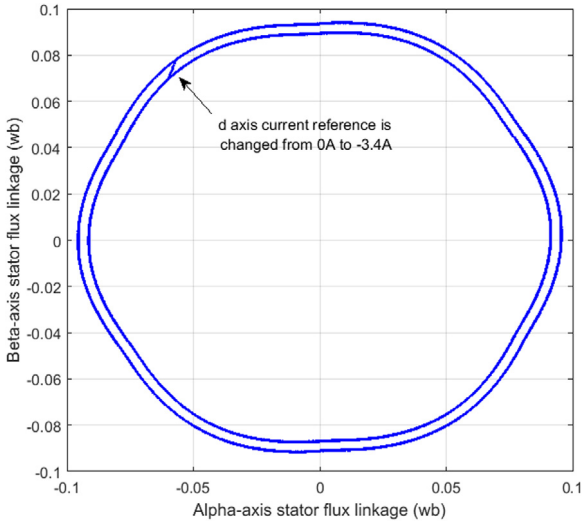

Fig. 7. Flux linkage trajectory of BLDCM is indirectly controlled by *d*-axis current at rated speed under 3.3 Nm load torque.

equal to 0.5 s. In Fig. 8(a) a comparison of efficiency in constant flux control system ($i_{ds}^{r*} = 0$) and proposed LMA is provided. It is clearly shown that the proposed LMA scheme improves the efficiency in the whole range of operation in comparison with traditional constant flux control system. Efficiency improvement is between 2% to 11%; however, as it was expected, the amount of improvement in efficiency is higher at lighter load conditions.

Fig. 8(b) indicates d*q*-axis currents. The performance of direct torque and indirect flux control scheme in suitable tracking of optimum *d*-axis current is shown. Moreover, there exist $6\theta_r$-dependent terms in *q*-axis current as discussed previously.

Phase current of BLDCM is shown in Fig. 8(c). What stands out in this figure, is three phase conduction mode of operation. In addition, although *d*-axis current magnitude increases, the phase current would not exceed its rated value.

Estimated iron, mechanical, resistive and total losses are indicated in Fig. 8(d). It can be observed in Fig. 8(b) that once LMA is applied, the algorithm changes i_{ds}^{r*} to find the point that sum of iron and mechanical loss equals to resistive loss. This operating point corresponds to the minimum loss condition.

6. Experimental results

Performance of the proposed loss model control of BLDCM is experimentally validated for a 200 W outer rotor prototype specified in Table 3. As depicted in Fig. 9, the experimental setup consists of a 200 W outer rotor BLDCM with trapezoidal back-EMF indicated in Fig. 10, coupled with a 250 W DC machine by a timing belt. The rotor position is detected through an incremental encoder with 1024 pulses per round, mounted on DC generator. An external rheostat is also connected to the DC generator for applying variable load conditions.

A DSP-based digital control board is employed for machine drive control. All parts of the digital control board, including following sections, are introduced briefly in Fig. 9. TMS320F28335 discrete signal processor board designed with Texas Instruments Co. for motor control application with 68 kB RAM and 512 kB ROM inside it, IGBT based inverter board with intelligent IGBT driver, HCPL 316J, which guarantees the electrical isolation between power and control system. Switching frequency of the inverter is 10 kHz with the dead time equal to 1 —s. The outputs of the DSP board are PWM logic signals fed to inverter switches. Stator phase currents are measured by three Hall-effect current sensors (LEM LA-55P) and phase voltages are measured by voltage sensors (LEM LV-25-P). Analog second-order low pass filters with cut-off frequency of around 2.6 kHz are used for filtering all measured voltage and current signals. All measured variables are fed back to the DSP through its A/D channel. DAC–PWM of DSP is employed to show calculated signals on the oscilloscope. For instance, the rotor speed is initially normalized for PWM port (i.e. transformed to range from −1 to 1) inside the DSP, then it is converted to an analog signal to be depicted on the oscilloscope via low pass filter. However, it produces some undesirable noise on indicated signals. Moreover an external DAC is linked to the DSP in order to bring out desired variables. Experimental results for both modified loss model validation and proposed minimum loss model control of BLDCM are presented in the following subsections.

6.1. Experimental validation of the modified loss model

The proposed modified loss model of BLDCM is evaluated under real conditions through various experimental tests. In this regard, BLDCM is used as generator coupled to DC motor which is directly connected to power supply; the DC motor speed can be tuned to desired value by armature voltage (V_{dc}) control. DC current (I_{dc}) is measured to determine the input power of setup (P_{in}^{dc}) by multiplying I_{dc} by V_{dc}. Input power of BLDCM could be obtained by subtracting resistive and mechanical loss of DC motor (P_{cu}^{dc}, P_{mech}^{dc})

Please cite this article as: A. Khazaee, H. Abootorabi Zarchi and G. Arab Markadeh Loss model based efficiency optimized control of brushless DC motor drive. ISA Transactions (2018), https://doi.org/10.1016/j.isatra.2018.10.046.

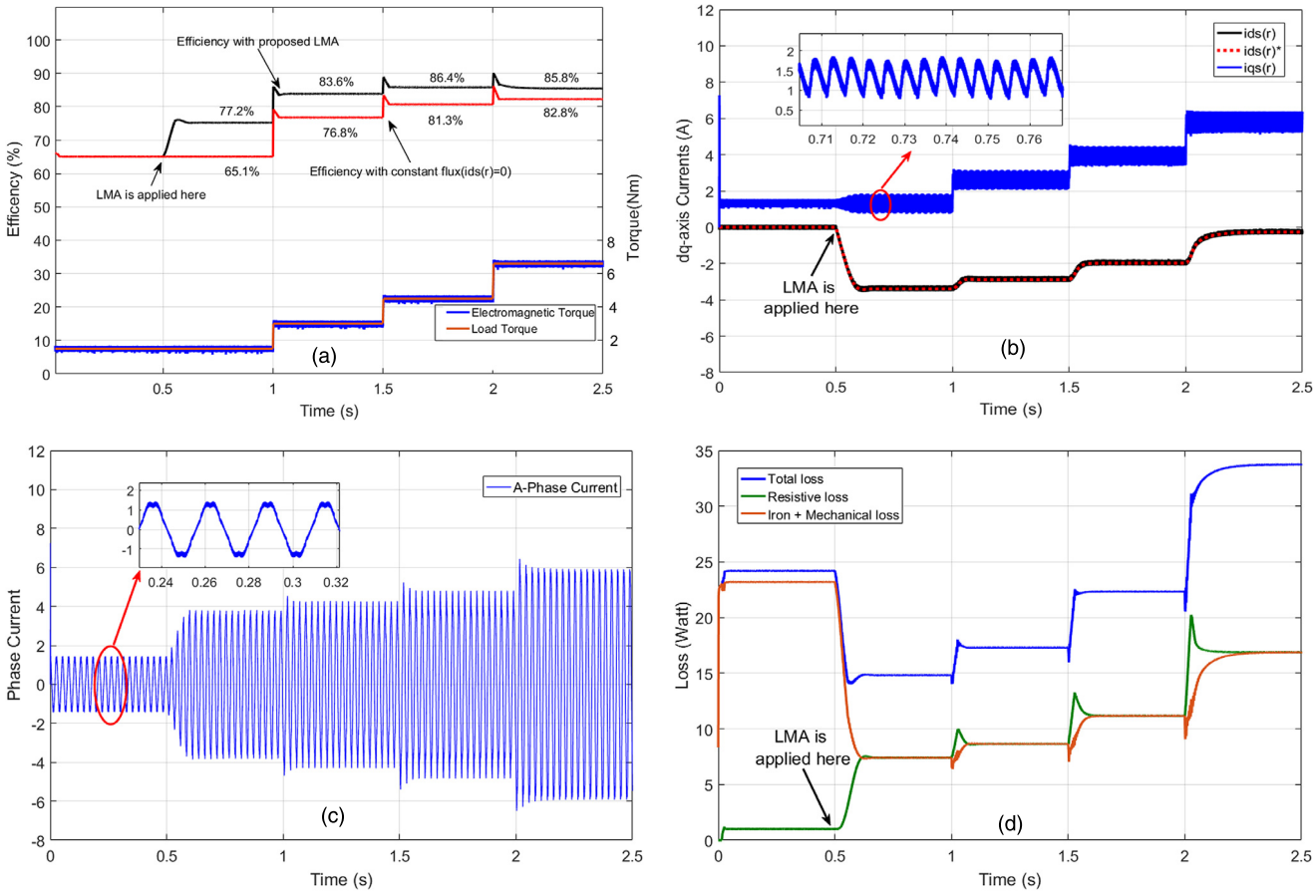

Fig. 8. Response of proposed LMA for step change in load at rated speed. (a): comparison of efficiency in constant flux and LMA. (b): dq axis currents. (c): Phase current. (d): Loss components.

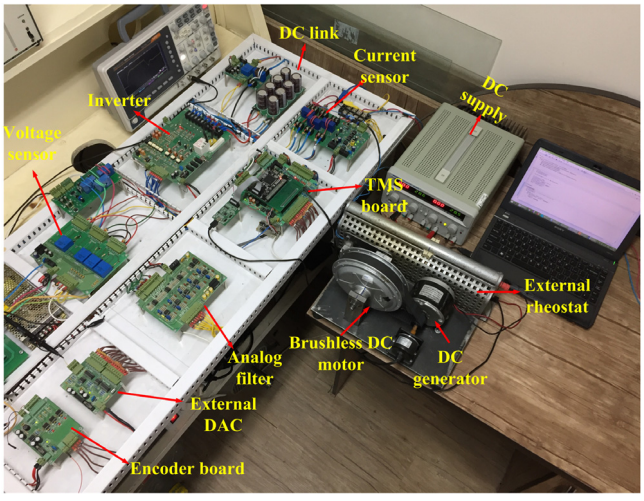

Fig. 9. The experimental setup of BLDCM.

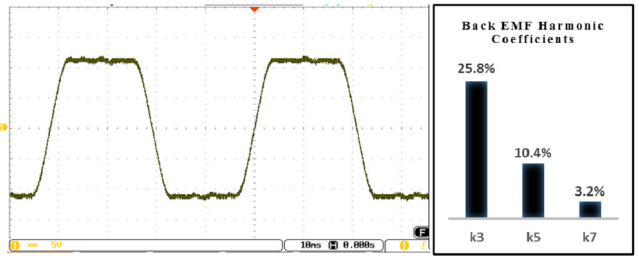

Fig. 10. Phase Back-EMF and its normalized harmonic coefficients at the speed of 18.7 rad/s.

from P_{in}^{dc}.

$$P_{in}^{BLDC} = P_{in}^{dc} - P_{Loss}^{dc} = V_{dc}I_{dc} - R_{dc}I_{dc}^2 - P_{rot}^{dc} \quad (27)$$

where R_{dc} is resistance of DC motor and P_{rot}^{dc} is sum of its mechanical and iron loss which is speed dependent and measured in no-load test of DC machine separated from drive train in different speeds.

Because of existence of back-EMF harmonics in order to improve accuracy of power loss, instantaneous output power of BLDCM ($p(t)$) is calculated in DSP, based on sensed stator voltages and currents

$$p(t) = p_a(t)+p_b(t)+p_c(t) = v_a(t)i_a(t)+v_b(t)i_b(t)+v_c(t)i_c(t) \quad (28)$$

where $p_a(t)$ denotes instantaneous power of A-phase. Fig. 11 shows three phase currents and $p_a(t)$. It can be observed that unlike the back-EMF, three phase currents do not contain third harmonic component.

The average value of $p(t)$ specifies output power of BLDCM (P_{out}^{BLDC}). Total loss and efficiency of BLDCM could be calculated as

$$P_{Loss}^{BLDC} = P_{in}^{BLDC} - P_{out}^{BLDC} \quad (29)$$

$$\eta_{BLDC} = \frac{P_{out}^{BLDC}}{P_{in}^{BLDC}}. \quad (30)$$

Please cite this article as: A. Khazaee, H. Abootorabi Zarchi and G. Arab Markadeh Loss model based efficiency optimized control of brushless DC motor drive. ISA Transactions (2018), https://doi.org/10.1016/j.isatra.2018.10.046.

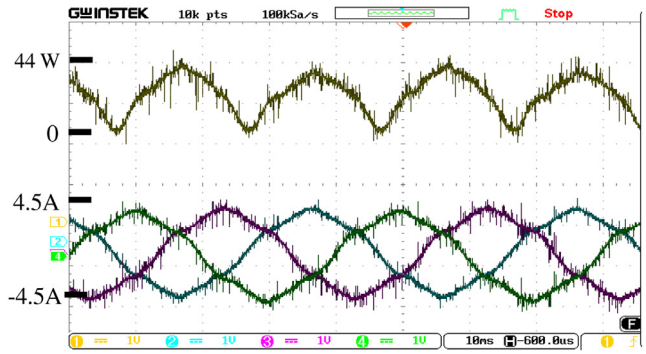

Fig. 11. Instantaneous power of A-phase (above) and three phase currents (below).

Table 4
Comparison of measured and estimated efficiency in different speeds under constant load resistor equals to at 3.6 Ω.

ω	P_{in}^{dc}	P_{loss}^{dc}	P_{out}^{BLDC}	η	η^{est}	Err
Rad/s	W	W	W	%	%	%
10	46.9	20.47	19.2	72.4	75.1	2.1
15	98.8	38.62	45.6	75.7	78.5	2.8
20	161.1	57.22	72.3	76.2	79.0	2.8
25	222.6	83.21	108	78.1	80.7	2.6
30	270	100.24	136.2	80.2	81.4	1.2

Table 5
Comparison of measured and estimated efficiency in different loads under constant rotational speed equals to 30 rad/s.

T_L	P_{in}^{dc}	P_{loss}^{dc}	P_{out}^{BLDC}	η	η^{est}	Err
Nm	W	W	W	%	%	%
0	35.8	2.76	0	–	–	–
1.28	73.5	10.17	38.4	60.6	63.0	2.4
2.38	124.1	25.28	71.37	72.2	74.1	1.9
4.54	270	100.24	136.2	80.2	81.4	1.2

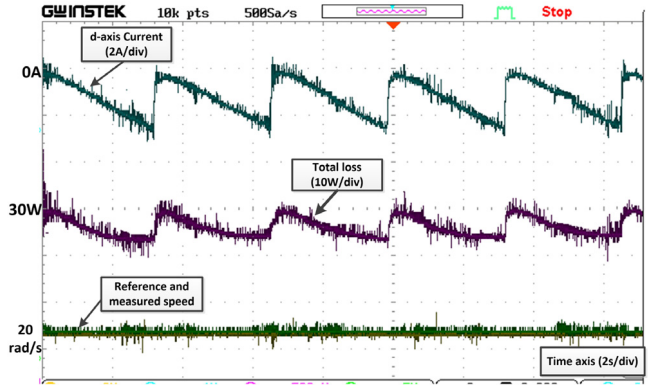

Fig. 12. Test results of control system for ramp reference of d-axis current from 0A to −3A at rated torque (6.6 Nm) where rotational speed reference kept constant at 20rad/s.

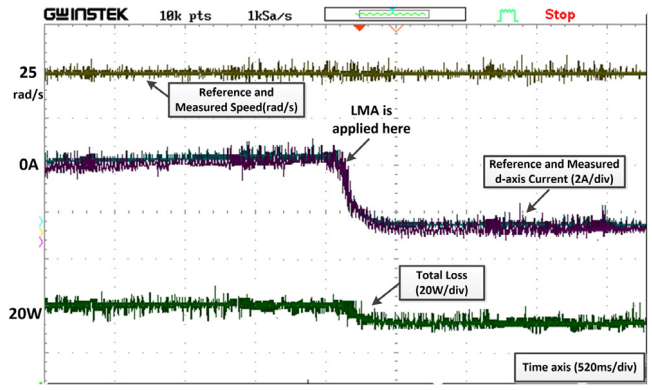

Fig. 13. Performance of proposed control system in loss minimization of BLDCM at 3.3 Nm where ω_m^* is kept constant at 25 rad/s.

The machine's efficiency is measured and compared with the estimated value in constant load resistor case under several speeds in Table 4. In addition, same results are provided under load variation in constant speed in Table 5. These results reveals that the error between the measured efficiency and estimated value obtained from modified loss model in Fig. 3 does not exceed 3%. This positive error can be a result of unmolded loss of machine. It can be also concluded that the modified loss model, which considers effects of back-EMF harmonics in iron and resistive loss, can provide an adequate insight to the machine's efficiency.

6.2. Experimental results of the proposed LMA

In this subsection experiments are performed to evaluate the proposed loss minimization algorithm. BLDCM is used as motor coupled with DC generator supplying an external rheostat for load variation as depicted in Fig. 9. Whole control system, indicated in Fig. 4, is implemented in a real-time PSIM model and downloaded to the TMS320F28335 employing Code Composer Studio software. Sample experimental results are presented below.

In order to show that there is an optimum value for d-axis current in which total loss of BLDCM is minimum, a ramp reference is applied to d-axis current while speed reference is kept constant at 20 rad/s. External rheostat is adjusted so that full load torque is applied. As it is demonstrated in Fig. 12, both rotational speed and d-axis currents are suitably tracking their reference values. Parabolic reduction of total loss in response to ramp reduction of d-axis current can be observed, implying existence of the optimum point corresponds to minimum loss condition. Therefore, it is feasible to reduce the loss of machine by controlling d-axis current. In this specified torque–speed condition for instance, there is an opportunity to reduce loss of machine by 6 W by controlling d-axis current at about 2.6 A. This optimum point could be obtained through the proposed method.

In order to compare total loss of BLDCM in constant flux and LMA control approaches, a further evaluation is conducted. The constant flux control is initially applied by setting d-axis current reference level to zero. Two seconds later, the LMA is applied and the proposed algorithm seeks for optimum d-axis current by introduced algorithm described in Fig. 6. The output of loss minimization algorithm is a desired value of d-axis current which is applied to control system while reference value of rotational speed is kept constant at 25 rad/s. 3.3 Nm load torque is applied by adjusting the rheostat. As depicted in Fig. 13, LMA successfully found the desired value of d-axis current. It can be also observed that any variation in d-axis current does not degrade the performance of speed control loop.

A sample test has been designed to compare the performance of proposed method with two other loss reduction techniques. The load torque is kept unchanged at 50% of rated i.e. 3.3 Nm while rotational speed reference steps up to 30 rad/s with a ramp function to assess startup performance. Afterward, it steps down to 15 rad/s and finally raises up to over nominal speed at 40 rad/s to evaluate over speed operation. This command is applied experimentally to three loss reduction methodologies to assess performance of control system and loss reduction capability in various conditions.

Please cite this article as: A. Khazaee, H. Abootorabi Zarchi and G. Arab Markadeh Loss model based efficiency optimized control of brushless DC motor drive. ISA Transactions (2018), https://doi.org/10.1016/j.isatra.2018.10.046.

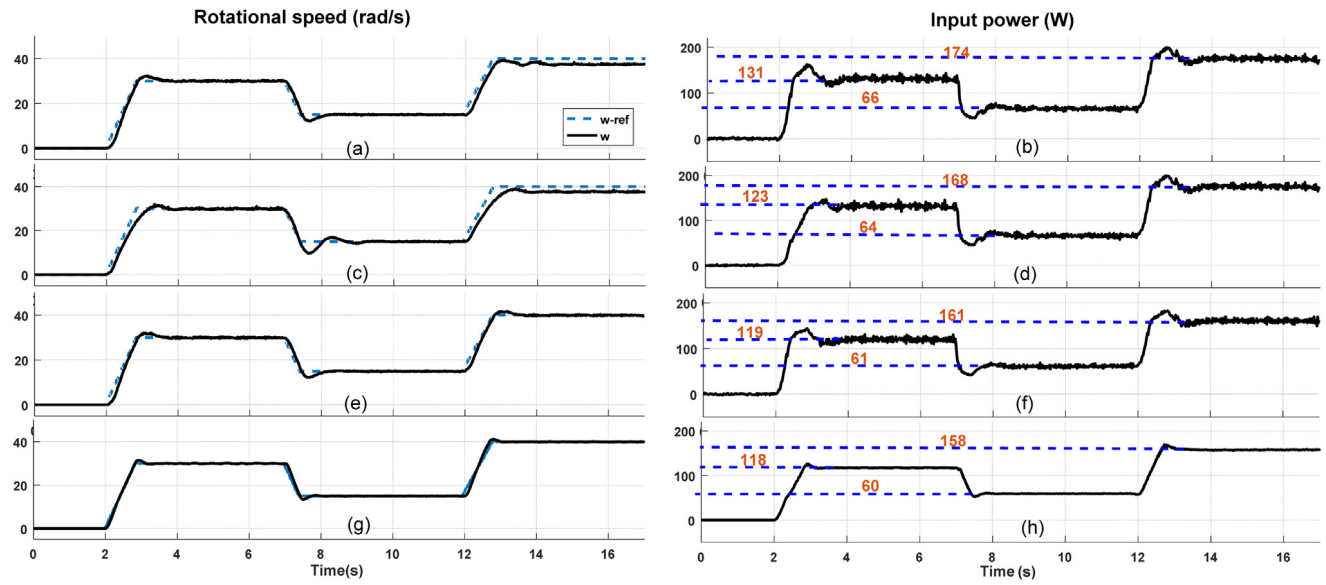

Fig. 14. Performance evaluation of proposed LMA in comparison with other techniques under 3.3 Nm load: (a), (b): experimental results of rotational speed and input power for MTPA; (c), (d): experimental results of rotational speed and input power for hybrid strategy; (e), (f): experimental results of rotational speed and input power for proposed LMA; (g), (h): simulation results of rotational speed and input power for proposed LMA.

First method is maximum torque per ampere (MTPA) approach which does not consider iron loss and operates at constant flux condition. Since *d*-axis current has no impact on torque production, the target expression is resistive loss minimization by controlling *d*-axis current at zero. In the second scheme introduced in [12], a hybrid control strategy is applied. In this method, non-sinusoidal harmonic injection scheme is used in the speed range until the sum of inverter conduction and stator resistive loss exceeds iron loss. When iron loss becomes dominant, the sinusoidal currents are preferred. The *d*-axis current has been kept constant at zero by vector control method leading to constant flux operation. Third method is proposed LMA in which flux linkage of machine is determined and controlled at its optimum value corresponding to minimum loss conditions.

The input power of setup for each method was computed from DC link voltage and current sensors. Moreover, it is filtered to remove switching frequency component and is depicted in second column of Fig. 14 for each method.

Fig. 14(a), (b) show the experimental results of MTPA implementation. It is clear in Fig. 14(a) that rotational speed is properly controlled in nominal range of operation. However the controller fails to track the reference at over speed operation.

Experimental results of rotational speed and corresponding input power for hybrid strategy is demonstrated in Fig. 14(c), (d) respectively. A comparison of required input power to supply specified torque–speed operation for MTPA (Fig. 14(b)) versus hybrid strategy (Fig. 14(d)) implies that input power has been reduced in all operating conditions due to hybrid current injection scheme. In the speed of 30 rad/s sinusoidal currents is injected; while in the speed of 15 rad/s non-sinusoidal harmonic current is preferred. Performance of controller degrades a little at 15 rad/s where strategy has changed current injection scheme. Moreover, such as MTPA, over speed operation cannot be feasible in this method. Therefore, if $i_{ds}^{*} = 0$, the desired torque can be only obtained under nominal speed.

Fig. 14(e), (f) represent the experimental results of the rotational speed and corresponding input power for proposed LMA. Analyzing Fig. 14(f) reveals that proposed LMA, requires minimum demanded input power in comparison with those for MTPA or hybrid strategy. This achievement is a result of removing extra iron loss which is produced due to unnecessary flux linkage, by controlling it at its optimum level. Regarding Fig. 14(e), a secondary outcome of flux reduction is that over speed operation could be achieved owing to flux weakening operation of machine. What stands out from this figure, motor is safely started that verifies the soft starting performance. Moreover, the proposed control system provides a proper response to step change in speed reference from 30 rad/s to 15 rad/s.

Finally this scenario has been simulated in order to provide a justification between simulation and experiments. Fig. 14(g), (h) demonstrate simulation results of rotational speed and required input power of proposed LMA respectively. The outcome endorse a minor difference in steady state values of input power through simulation and experimental results which can be a result of real component impacts and un-modeled losses.

Experimental results in this section reveal that applying LMA improves the efficiency of BLDCM without considerable influence on the performance of the control system.

7. Conclusions

This paper proposed a 'loss minimization algorithm' for BLDCM. In order to minimize the loss of BLDCM, the flux linkage is indirectly controlled by *d*-axis current. The LMA determines the optimum value of *d*-axis current corresponds to minimum loss condition. Since the loss model of PMSM is validated only in sinusoidal back-EMF, it is not precise to use it for BLDCM with trapezoidal back-EMF. Therefore, modified loss model of BLDCM has been developed in the current work. The proposed modified loss model extends multiple reference frame theory and can be used to take the back-EMF harmonics and variation of iron loss resistance into account. This model has been verified through the experimental tests and is applied in the control system . The performance of the proposed DTC based LMA in efficiency improvement of BLDCM has been judged under several operating points through experimental and simulation tests. Efficiency improvement is more significant in lighter load conditions and hence it can be a suitable choice to use this control scheme in industrial and renewable energy applications such as solar water pumping systems. Moreover, as a result of operation of BLDCM at flux weakening region in the proposed LMA, high speed operation can be feasible.

Please cite this article as: A. Khazaee, H. Abootorabi Zarchi and G. Arab Markadeh Loss model based efficiency optimized control of brushless DC motor drive. ISA Transactions (2018), https://doi.org/10.1016/j.isatra.2018.10.046.

References

[1] Bazzi AM, Krein PT. Review of methods for real-time loss minimization in induction machines. IEEE Trans Ind Appl 2010;46:2319–28.
[2] Thirusakthimurugan P, Dananjayan P. A novel robust speed controller scheme for PMBLDC motor. ISA Trans 2007;46:471–7.
[3] Feng G, Lai C, Kar NC. Practical testing solutions to optimal stator harmonic current design for pmsm torque ripple minimization using speed harmonics. IEEE Trans Power Electron 2018;33:5181–91.
[4] Shirvani Boroujeni M, Arab Markadeh GR, Soltani J. Torque ripple reduction of brushless dc motor based on adaptive input–output feedback linearization. ISA Trans 2017;70:502–11.
[5] Masmoudi M, El Badsi B, Masmoudi A. Direct Torque Control of Brushless DC Motor Drives With Improved Reliability. IEEE Trans Ind Appl 2014;50:3744–53.
[6] Kooning JD, JVd Vyver, Meersman B, Vandevelde L. Maximum Efficiency current waveforms for a PMSM including iron losses and armature reaction. IEEE Trans Ind Appl 2017. 1-.
[7] Shabanian A, Tousiwas AAP, Pourmandi M, Khormali A, Ataei A. Optimization of brushless direct current motor design using an intelligent technique. ISA Trans 2015;57:311–21.
[8] Hanselman. Minimum torque ripple DC. Maximum efficiency excitation of brushless permanent magnet motors. IEEE Trans Ind Electron 1994;41:292–300.
[9] Aghili F, Buehler M, Hollerbach JM. Experimental characterization and quadratic programming-based control of brushless-motors. IEEE Trans Control Syst Technol 2003;11:139–46.
[10] Aghili F. Optimal feedback linearization control of interior PM synchronous motors subject to time-varying operation conditions minimizing power Loss. IEEE Trans Ind Electron 2018;65:5414–21.
[11] Sung-Jun P, Han Woong P, Man Hyung L, Harashima F. A new approach for minimum-torque-ripple maximum-efficiency control of BLDC motor. IEEE Trans Ind Electron 2000;47:109–14.
[12] Kshirsagar P, Krishnan R. High-Efficiency current excitation strategy for variable-speed nonsinusoidal back-EMF PMSM machines. IEEE Trans Ind Appl 2012;48:1875–89.
[13] Uddin MN, Zou H, Azevedo F. Online loss-minimization-based adaptive flux observer for direct torque and flux control of PMSM drive. IEEE Trans Ind Appl 2016;52:425–31.
[14] Tripathi SM, Dutta C. Enhanced efficiency in vector control of a surface-mounted pmsm drive. J Franklin Inst 2018;355:2392–423.
[15] Cavallaro C, Di Tommaso AO, Miceli R, Raciti A, Galluzzo GR, Trapanese M. Efficiency enhancement of permanent-magnet synchronous motor drives by online loss minimization approaches. IEEE Trans Ind Electron 2005;52:1153–60.
[16] Ozturk SB, Toliyat HA. Direct torque and indirect flux control of brushless dc motor. IEEE/ASME Trans Mechatronics 2011;16:351–60.
[17] Ozturk SB, Toliyat HA. Direct Torque Control of Brushless DC Motor with Non-sinusoidal Back-EMF. In: 2007 IEEE international electric machines & drives conference 2007. pp. 165-71.
[18] Chapman PL, Sudhoff S, Whitcomb C. Multiple reference frame analysis of non-sinusoidal brushless DC drives. IEEE Trans Energy Convers 1999;14:440–6.
[19] Tabarraee K, Iyer J, Atighechi H, Jatskevich J. Dynamic average-value modeling of 120° VSI-commutated brushless DC motors with trapezoidal back EMF. IEEE Trans Energy Convers 2012;27:296–307.
[20] Yamazaki K. Torque and efficiency calculation of an interior permanent magnet motor considering harmonic iron losses of both the stator and rotor. IEEE Trans Magn 2003;39:1460–3.
[21] Fernandez-Bernal F, Garcia-Cerrada A, Faure R. Determination of parameters in interior permanent-magnet synchronous motors with iron losses without torque measurement. IEEE Trans Ind Appl 2001;37:1265–72.
[22] Morimoto S, Tong Y, Takeda Y, Hirasa T. Loss minimization control of permanent magnet synchronous motor drives. IEEE Trans Ind Electron 1994;41:511–7.
[23] Gyu-Sik K, In-Joong H, Myoung-Sam K. Control of induction motors for both high dynamic performance and high power efficiency. IEEE Trans Ind Electron 1992;39:323–33.
[24] Li H, Ning X, Li W. Implementation of a MFAC based position sensorless drive for high speed BLDC motors with nonideal back EMF. ISA Trans 2017;67:348–55.
[25] Chen S, Luo Y, Pi Y. PMSM sensorless control with separate control strategies and smooth switch from low speed to high speed. ISA Trans 2015;58:650–8.
[26] Azevedo FCF, Uddin MN. Recent advances in loss minimization algorithms for IPMSM drives. In: 2014 IEEE industry application society annual meeting 2014. pp. 1-9.

Please cite this article as: A. Khazaee, H. Abootorabi Zarchi and G. Arab Markadeh Loss model based efficiency optimized control of brushless DC motor drive. ISA Transactions (2018), https://doi.org/10.1016/j.isatra.2018.10.046.